Reactivity of HNC with Small Hydrocarbon Radicals

Simon Petrie*

School of Chemistry, University College, Australian Defence Force Academy, University of New South Wales, Canberra ACT 2600 Australia, and Chemistry Department, The Faculties, Australian National University, Canberra ACT 0200 Australia

Received: April 15, 2002; In Final Form: August 2, 2002

We report a theoretical study of the potential energy surfaces relevant to reaction of hydrogen isocyanide (HNC) with the hydrocarbon radicals R (R = H, CH_3, C_2H, C_2H_3, C_2H_5). Stationary points on these surfaces have been obtained at the B3-LYP/6-311+G** level of theory; relative energies of the stationary points have been determined by implementation of the CBS-RAD "model chemistry" methodology on the B3-LYP/6-311+G** optimized geometries. Product channels considered are nitrile formation (RCN + H), R-catalyzed tautomerization (HCN + R), and, when exothermic, H-atom abstraction (RH + CN). We find that the barriers to the HCN + R channel universally exceed those for the RCN + H channel, thus effectively inhibiting the former process at low temperatures. Nevertheless (with the exception of R=C_2H), a moderate barrier (E_a < 35 kJ mol^{-1}) also exists to RCN + H production. The comparatively low reactivity thus inferred for HNC, in the context of its reactions with radicals in general, is consistent with the apparent longevity of HNC in cold astrophysical environments, which contain such radicals. However, none of the reactions surveyed here seems to fulfill the requirements of the unidentified "200 K" barrier to HNC removal in interstellar clouds.

Introduction

Despite its instability under laboratory conditions, hydrogen isocyanide (HNC) is a remarkably widespread molecule. HNC has been detected in such diverse molecular astrophysical environments as diffuse interstellar clouds,[1,2] prestellar disks,[3,4] outflowing circumstellar envelopes,[5,6] and planetary nebulae;[7,8] it is particularly prevalent in the cores of cold, dense interstellar clouds,[9−11] where its abundance is often found to substantially exceed that of the more conventional isomer HCN.[10] Closer to Earth, HNC is frequently detected within cometary comae[12−18] and has recently been proposed as a trace constituent of the upper atmosphere of the large Saturnian moon Titan.[19] In most of these environments, the predominant mechanism for HNC formation appears to be via the dissociative recombination of the $HCNH^+$ parent ion:

$$HCNH^+ + e \rightarrow HCN + H \quad (1a)$$

$$\rightarrow HNC + H \quad (1b)$$

$$\rightarrow CN + (2H \text{ or } H_2) \quad (1c)$$

Despite the intrinsic difficulties inherent in the study of such dissociative recombination processes, reaction 1 has now been subjected to several detailed high-level ab initio studies[20−23] and has recently also received experimental attention.[24] It is now reasonably well-accepted that HNC + H is an important product channel in reaction 1 and may even dominate over the other channels. Nonetheless, while much is currently known of the formation and distribution of HNC within extraterrestial environments, very little is known of its removal through subsequent reactions. No direct experimental studies of HNC reactions appear to have yet been reported, although a combined experimental/theoretical study has suggested[25] that rapid oxidation of HNC by OH and by O is necessary to explain the observed kinetics of HCN reactivity in shock-tube studies. Aside from its reactivity with OH and O,[25] the only reactions of HNC to have been explicitly investigated theoretically are the processes

$$HNC + H \rightarrow HCN + H \quad (2)$$

and

$$HNC + C_2H \rightarrow HCCCN + H \quad (3)$$

Both reactions are exothermic: reaction 2 is found to possess a significant activation barrier,[26,27] while reaction 3 is barrierless[28] and hence constitutes an important route to HCCCN within interstellar clouds. A further process

$$HNC + CH_3 \rightarrow CH_3CN + H \quad (4)$$

while not having been the specific focus of previous work, has in effect been characterized since the potential energy surface of the reverse process has recently been reported.[29] Consequently, it appears also that reaction 4 possesses a moderate activation barrier. The selectivity typified by reactions 2−4 does not merely explain the detectability of interstellar HNC (rapid occurrence of reaction 2 would very likely reduce HNC below the detection limit in most objects, since H is a particularly abundant interstellar species); it serves to indicate also that a clear understanding of HNC's reactivity will require close examination of many potential reactions of this species. Further motivation for the study of HNC's reactivity is provided by the suggestion[10] that an as yet unidentified process possessing a ∼200 K (1.7 kJ mol^{-1}) barrier is central to the apparent destruction of HNC in warm molecular astrophysical environments. This proposal is based on the observation[10] of a

* To whom correspondence should be addressed. E-mail: spetrie@rsc.anu.edu.au.

10.1021/jp025947x CCC: $22.00
Published on Web 10/22/2002

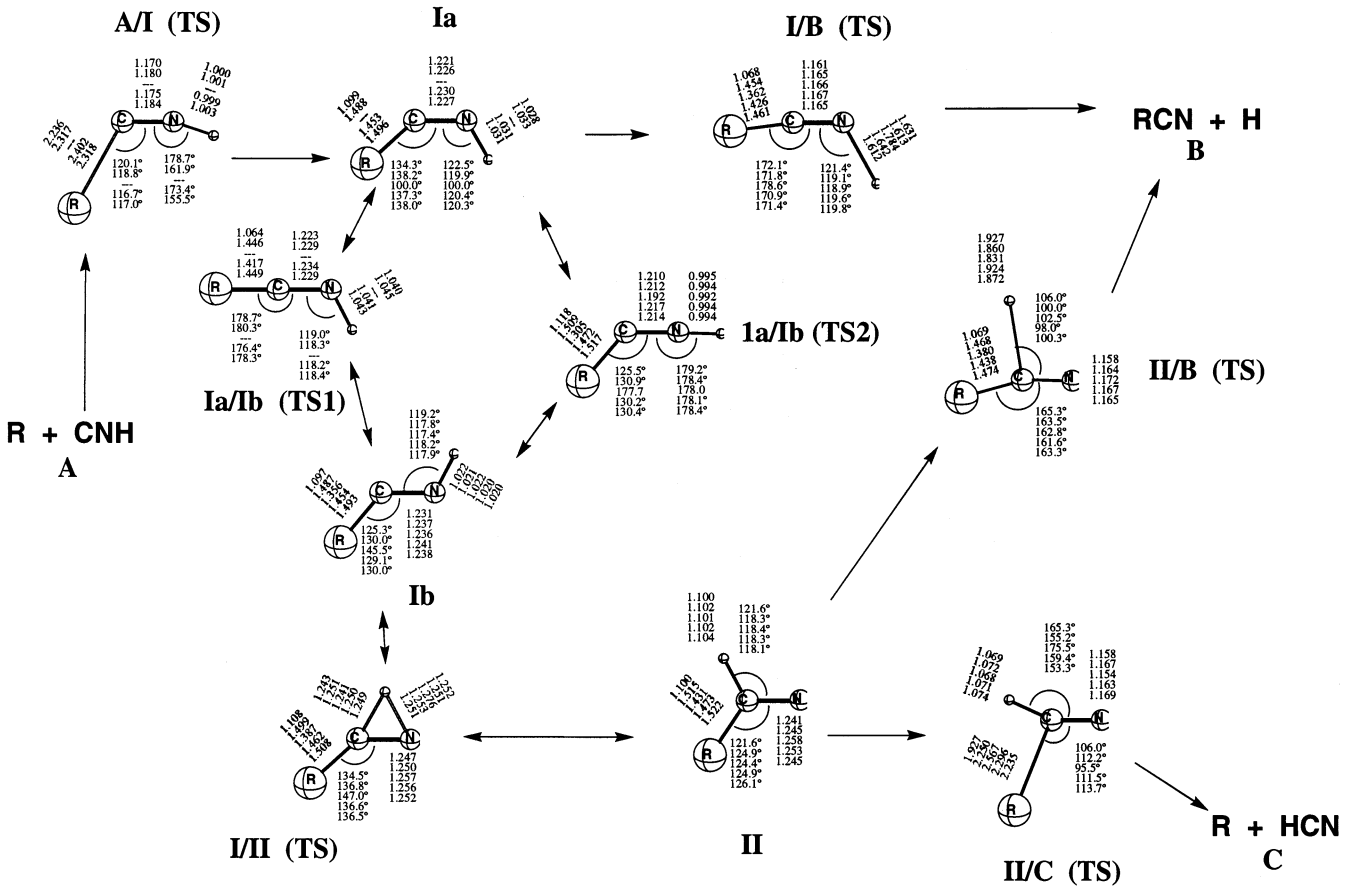

Figure 1. B3-LYP/6-311+G** optimized geometries of stationary points. Bond lengths (in Ångstroms) and bond angles (in degrees) are listed, respectively, for R = H, CH_3, C_2H, C_2H_3, and C_2H_5.

systematic reduction in the HNC/HCN abundance ratio with increasing temperature in a wide-ranging survey of interstellar environments. Because the experimental difficulties, which beset kinetic evaluation of HNC's reactivity, are considerable, computational tools such as ab initio quantum chemical calculations may reasonably be considered to be the method of choice for such evaluation. In the present work, we reexamine reactions 2−4 and evaluate also the prospects for reaction of HNC with the C_2H_3 and C_2H_5 radicals, using the CBS-RAD procedure.

Theoretical Methods

The potential energy surfaces (PES) investigated herein have been characterized at the B3-LYP/6-311+G** level of theory; in some cases, identified within the text, optimizations at the QCISD/6-31G* level of theory were also employed to assess the suitability of the B3-LYP hybrid density functional method (which has been previously recommended as a very economical computational method for characterizing molecular radicals)[30] for the species of interest in the present work. After geometry optimization, single-point total energies were determined using the CBS-RAD technique developed by Radom and co-workers. This computational technique, which is described in detail elsewhere,[31] is designed to obviate problems of spin contamination, which are known to affect the accuracy of calculations on CN-containing radicals. The main objective of the CBS-RAD method is to deliver, for radicals, structural and thermochemical data of comparable accuracy to that typically attained for closed shell systems using more general "model chemistry" methods such as the CBS-Q procedure,[32] on which CBS-RAD is reasonably closely modeled. The Radom group have very recently reported[33] an appraisal of the performance of CBS-RAD and of many other model chemistry approaches in calculations on small open shell molecules. Their study finds generally small (and nonsystematic) differences between the calculated CBS-Q and CBS-RAD enthalpies of formation; it is, however, notable that the most highly spin-contaminated radicals included in their test set (the doublets CN, CS^+, and C_2H, all with $<S^2> < 1.0$) are all significantly better treated by CBS-RAD than by CBS-Q, as diagnosed by the respective errors in calculated $\Delta H_{f,0}°$ values delivered by the two methods.[33] In the context of potential energy surface exploration where the degree of spin contamination can vary considerably between neighboring stationary points, this suggests that CBS-RAD is a more "robust" method than CBS-Q. All calculations in the present work were performed using the GAUSSIAN98 programming suite.[34]

Results and Discussion

Generalized RCNH Potential Energy Surface. In Figure 1, we present a generalized depiction of the important stationary points for the reaction channels

$$R + CNH \rightarrow RCN + H \quad (5)$$

and

$$R + CNH \rightarrow R + HCN \quad (6)$$

with bond lengths and angles shown for the lowest-energy conformers[35] in each instance. While the energetic profiles of the different surfaces can vary widely, as discussed in detail in subsequent sections, it is also readily apparent from the figure that for many of the stationary points, the geometry of the (H,

TABLE 1. Total Energies for Stationary Points on the [H + HNC] Potential Energy Surface at the CBS-RAD Level of Theory

species	ZPE[a] (mHartree)	i[b]	$<S^2>$[c]	E_0[d] (Hartree)	E_{rel}[e] (kJ mol^{-1})	lit[f] (kJ mol^{-1})
R + CNH (**A**)			0.75		0	0
A/I (TS)	16.06	1	0.76	−93.76079	8.0	17.6[g], 13.8[h]
Ia	24.74	0	0.83	−93.80629	−111.5	−105.0[h]
Ia/Ib (TS1)	23.08	1	0.83	−93.78978	−68.1	
Ia/Ib (TS2)	22.91	1	0.77	−93.79061	−70.3	−62.3[h]
Ib	25.74	0	0.82	−93.81311	−129.4	−109.2[g], −123.4[h]
I/B (TS)	16.93	1	0.88	−93.77161	−20.4	9.2[g], −9.6[h]
RCN + H (**B**)			0.75		−58.8	−63.6[g], −60.2[h]
I/II (TS)	19.72	1	0.79	−93.75345	27.3	31.0[h]
II	25.05	0	0.94	−93.82636	−164.1	−157.7[h]
II/B (TS)	17.27	1	0.91	−93.77759	−36.1	−23.8[h]

[a] ZPE (uncorrected) at the B3-LYP/6-311G** level of theory. [b] Number of imaginary vibrational frequencies, according to B3-LYP/6-311G** calculations. [c] Expectation value, indicating the magnitude of spin contamination ($<S^2> = 0.75$ for pure doublet). [d] Total CBS-RAD energy (at 0 K) including ZPE.[31] [e] Energy relative to the reactants H + HNC, at 0 K, according to CBS-RAD calculations. [f] Relative energies (referenced to R + HNC), obtained from previous ab initio studies as indicated. [g] MP4/6-311++(3df,2p)//MP3/6-311++G(d,p) values, reported in ref 26. [h] CCSD(T)/6-311++(3df,3pd)//CCSD(T)/6-311++G(d,p) values, reported in ref 27.

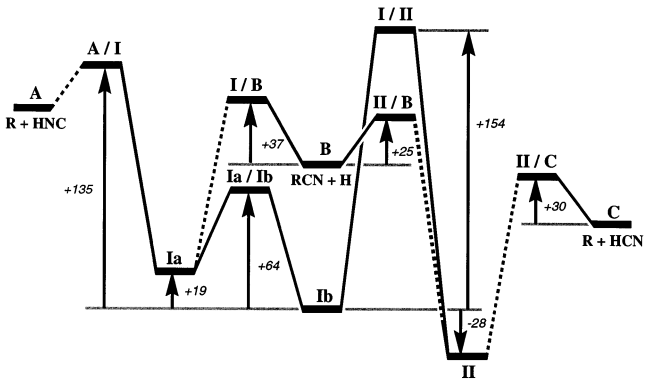

Figure 2. Generalized potential energy diagram (all relative energy values in kJ mol^{-1}) for reactions of (saturated) hydrocarbon radicals R with HNC.

N, C) moiety is almost invariant across the sequence of R radicals surveyed here.

Common qualitative features of the different surfaces, at the B3-LYP/6-311+G** level, may be summarized as follows. For all R except C_2H, a barrier impedes formation of the RCNH intermediate (**I**) from reactants R + CNH (**A**). Again except for R = C_2H, there are two distinct (cis and trans) stereoisomers of **I**, for which two direct pathways for interconversion can be identified by inversion of either the RCN or the CNH bond angle. H loss from **I** to form RCN + H (**B**) is universally barrier-inhibited. Both the reaction entrance channel (**A**/**I**) and the **I**/**B** product channel occur via the cis isomer **Ia** and not the trans isomer **Ib** (except for R=C_2H, for which **Ia** is not a stationary point). Tautomerization of **Ib** to form RC(H)N, **II**, is impeded by a barrier, and barriers also exist to both R loss (yielding HCN + R) and H loss (to RCN + H) from **II**.

The B3-LYP/6-311+G** calculations provide optimized geometries, but relative energies obtained at this level are not expected to be highly reliable. When the CBS-RAD technique is implemented on these optimized geometries, we obtain relative energies, which should offer a clearer picture of the true PES for each system. While the high-level results for each surface are discussed in detail in the following subsections, it may prove instructive at this juncture to construct a "generalized" R + HNC potential energy surface, as embodied in Figure 2. We can consider such a surface to be divided into four "zones", the first zone being that of the reactants (**A**, R + HNC); second, the entrance channel transition state and subsequent reactive intemediates RC(H)N; third, the dissociating RCN + H (**B**) products; and fourth, the competing product channel (**C**) of dissociation to R + HCN. Within any of these zones, the relative energies defined in Figure 2 are virtually unchanged (within a margin of ±5 kJ mol^{-1}) on substitution of R = H by R = CH_3 or C_2H_5, suggesting that the reactivity of yet larger "saturated" radicals with HNC may also be usefully predicted from such a surface.

Please note also that in our exploration of the PES for each system, we have investigated in detail only that portion of the PES that is most directly accessible by radical addition at the terminal C atom. Reaction may also feasibly occur by addition at N, producing an intermediate CN(H)R with carbene and radical character, but our calculations show that this pathway is consistently impeded by a much higher barrier than that associated with addition at C. Furthermore, the N attack path would appear to lead predominantly to RNC formation (by H loss) in the first instance, and high-level calculations have shown[19] that such a product channel is exothermic only in the instance of R=C_2H, for which our assignment of a substantial intervening barrier is supported by a previous high-level study.[28]

Reaction of H with HNC. Our results for this PES are summarized in Table 1. The HCNH potential energy surface has been explored previously by Talbi et al.[26] and by Sumathi and Nguyen.[27] The initial study of Talbi et al.[26] employed calculations at levels up to MP4/6-311++G(3df,2pd)//MP3/6-311++G**, while the work of Sumathi and Nguyen[27] used CCSD(T)/6-311++G(3df,3pd)//CCSD(T)/6-311++G** calculations. As well as utilizing a more computationally demanding level of theory, the latter study is also more comprehensive in its characterization of stationary points upon the (doublet) potential energy surface, reporting minima for **II** and CNH_2 as well as for the two stereoisomers of HCNH, **Ia** and **Ib**. In contrast, the study of Talbi et al.[26] features only (*E*)-HCNH (**Ib**) as an intermediate; note, however, that the transition structures identified on the entrance (H + HNC) and exit (H + HCN) channels in the study of Talbi et al.[26] are those which Sumathi and Nguyen[27] have identified with the (*Z*)-HCNH intermediate (**Ia**), which in the latter study provides the most straightforward pathway to H + HCN. Interconversion of **Ia** and **Ib** is facile according to the latter study, through an inversion of the HCN bond angle (which we identify as the **Ia**/**Ib** (TS1) transition structure); this inversion process is energetically accessible to the HNC + H reactants but serves principally as a "bottleneck" since **Ib** does not directly dissociate to HCN + H, instead leading to H_2CN via a barrier-inhibited isomerization (31 kJ mol^{-1} above reactants as compared to our value of 27.3 kJ mol^{-1} for the same barrier height). In the present work, we have

TABLE 2. Dependence of Some Transition State Structures on Optimized Geometry

R	TS	parameter	B3-LYP/6-311+G**	QCISD/6-31G*	QCISD/6-311+G**
H	**A/I**	r(H−C)	2.24 Å	1.77 Å	1.85 Å
		$<S^2>$	0.76	0.80	0.78
		E_{rel}[a]	8.0 kJ mol^{-1}	11.2 kJ mol^{-1}	12.9 kJ mol^{-1}
H	**I/B**	r(N−H)	1.63 Å	1.50 Å	1.53 Å
		$<S^2>$	0.88	0.99	0.95
		E_{rel}[a]	−20.4 kJ mol^{-1}	−19.2 kJ mol^{-1}	−18.5 kJ mol^{-1}
H	**I/II**	r(C−H)	1.24 Å	1.25 Å	1.24 Å
		r(N−H)	1.25 Å	1.26 Å	1.26 Å
		$<S^2>$	0.79	0.80	0.79
		E_{rel}[a]	27.3 kJ mol^{-1}	27.4 kJ mol^{-1}	27.4 kJ mol^{-1}
H	**II/B**	r(C−H)	1.93 Å	1.76 Å	1.81 Å
		$<S^2>$	0.91	1.04	1.00
		E_{rel}[a]	−36.1 kJ mol^{-1}	−35.1 kJ mol^{-1}	−34.9 kJ mol^{-1}
CH_3	**A/I**	r(C−C)	2.32 Å	2.19 Å	
		$<S^2>$	0.79	0.81	
		E_{rel}[a]	30.5 kJ mol^{-1}	31.2 kJ mol^{-1}	
CH_3	**I/B**	r(N−H)	1.61 Å	1.49 Å	
		$<S^2>$	0.85	0.96	
		E_{rel}[a]	−9.3 kJ mol^{-1}	−8.2 kJ mol^{-1}	
C_2H	**A/I**	r(C−C)		2.52 Å	
		$<S^2>$		1.17	
		E_{rel}[a]		−11.6 kJ mol^{-1}[b]	
C_2H_3	**A/I**	r(C−C)	2.40 Å	2.22 Å	
		$<S^2>$	0.96	1.01	
		E_{rel}[a]	16.6 kJ mol^{-1}	16.0 kJ mol^{-1}	

[a] Energy relative to the reactants R + HNC at 0 K, evaluated using the CBS-RAD E_e value for the transition state geometry optimized at the level of theory shown. Note, however, that to facilitate interpretation of the transition state's total energy upon the optimization method, the reactant R and HNC CBS-RAD energies used here are those obtained using the B3-LYP/6-311+G** geometries. Furthermore, for computational expediency, the transition state ZPE value used is always the B3-LYP value. [b] Using a ZPE value of 30.00 mHartrees for this TS, obtained from the scaled (0.92) HF/6-31G* value.

identified a second stereoisomerization pathway, viz. **Ia/Ib** (TS2), between the two HCNH structures, by HNC bond angle inversion: the energetic requirements of the two HCNH interconversion processes are similar, and both lie fully submerged below the reactant energy according to our CBS-RAD calculations. The most critical energetic parameter in dictating the reaction kinetics, i.e., the height of the entrance channel barrier, is determined to be 17.7 (Talbi et al.),[26] 13.8 (Sumathi and Nguyen),[27] and 8.0 kJ mol^{-1} (this work): thus, while there is some disageement regarding the precise height of the barrier, all three studies concur that the barrier exceeds the total energy of the reactants and will therefore effectively prevent occurrence of the overall reaction at low temperatures.

Comparison of our results with the detailed PES of Sumathi and Nguyen[27] shows that there is generally a close accord between the two sets of values. It is notable that the worst discrepancies are seen for transition states with the highest degree of spin contamination, i.e., **I/B** and **II/B**, for which our CBS-RAD values lie more than 10 kJ mol^{-1} below the corresponding CCSD(T) values of the earlier study.[27] This would appear to reflect (a) the tendency of CBS-RAD to additionally stabilize highly spin-contaminated structures, via the ΔE_{spin} correction term,[31] in a manner that is not implemented in single-point CCSD(T) calculations and/or (b) the apparent tendency of the B3-LYP method to deliver comparatively poor geometries for dissociative transition states.[36−38]

The influence of the method of geometry optimization on the resultant CBS-RAD total energies can be gauged from the structural and energetic values reported in Table 2. Here, we have reoptimized the crucial transition state structures at the QCISD/6-31G* and QCISD/6-311+G** levels of theory and have compared the CBS-RAD energies (excluding zero-point energy (ZPE)) obtained from these geometries with those yielded by our "default" B3-LYP/6-311+G** structures. It is apparent, from Table 2, that for transition states involving dissociation to bimolecular products, the saddle point for bond cleavage occurs at consistently larger separations according to B3-LYP/6-311+G** than for QCISD/6-31G*, with QCISD/6-311+G** critical bond lengths lying somewhat between these two extremes but generally closer to QCISD/6-31G*. The QCISD/6-311+G** values generally also show the closest accord with the more computationally intensive CCSD(T)/6-311++G** method employed by Sumathi and Nguyen.[27] We can surmise that the B3-LYP/6-311+G** method therefore tends to overestimate the critical bond lengths in the dissociative transition states (a conclusion which is broadly consistent with previous studies). However, this apparent bond length overestimation does not greatly impact the resultant CBS-RAD energies, with the greatest range in total energies corresponding to less than 5 kJ mol^{-1} (for the R = H **A/I** transition state) across the three optimization methods surveyed in Table 2, despite H−C bond lengths for this example that range from 1.77 (QCISD/6-31G*) to 2.24 Å (B3-LYP/6-311+G**). Note also that B3-LYP/6-311+G** appears to consistently yield the lowest, and QCISD/6-31G* the highest, degree of spin contamination in the optimized transition states (as judged via the $<S^2>$ values obtained in the UMP2/CBSB3 single-point calculation); this tendency will act to mitigate the energy discrepancy between different optimization methods in the resultant CBS-RAD values, due to the action of the CBS-RAD ΔE_{spin} correction factor.[31] Nonwithstanding this spin correction effect, it appears also that our default B3-LYP/6-311+G** geometries will generally lead to a slight underestimation of the barrier heights. While this conclusion does not materially affect the qualitative agreement between our results and the high-level calculations of Sumathi and Nguyen[27] (i.e., a significant barrier on the H + CNH entrance channel but no absolute barrier to the direct HCN + H exit channel), it must necessarily inform our assessment of the PES for the reactions of the hydrocarbon radicals CH_3,

TABLE 3. Total Energies for Stationary Points on the [CH_3 + HNC] Potential Energy Surface at the CBS-RAD Level of Theory

species	ZPE[a] (mHartree)	i[a]	$<S^2>$[a]	E_0[a] (Hartree)	E_{rel}[a] (kJ mol^{-1})	lit[a,b] (kJ mol^{-1})
R + CNH (**A**)			0.76		0	0
A/I (TS)	47.85	1	0.79	−132.99610	30.5	34.7
Ia[c]	53.92	0	0.81	−133.04079	−86.8	−82.8
Ia/Ia (TS)[d]	53.49	1	0.82	−133.03980	−84.3	
Ia/Ib (TS1)	51.22	1	0.81	−133.02271	−39.4	
Ia/Ib (TS2)	52.75	1	0.77	−133.02287	−39.8	−33.9
Ib[c]	54.86	0	0.81	−133.04814	−106.1	−101.7
Ib/Ib (TS)[d]	54.44	1	0.81	−133.04735	−104.1	
I/B (TS)	45.96	1	0.85	−133.01126	−9.3	−6.3
RCN + H (**B**)			0.75		−45.6	−46.4
I/II (TS)	49.33	1	0.79	−132.98990	46.8	51.0
II	54.45	0	0.91	−133.05746	−130.6	−126.8
II/B (TS)	46.74	1	0.90	−133.01447	−17.7	−14.6
II/C (TS)	49.04	1	0.99	−133.01641	−22.8	−19.2
R + HCN (**C**)			0.76		−58.8	−60.7

[a] See footnotes *a*−*f* for Table 1. [b] Relative energies (referenced to R + HNC), obtained using the G3 method with B3-LYP/6-311++G(2d,2p) optimized geometries, reported in ref 29. [c] Local minimum features an eclipsed interaction of the in-plane methyl H−C bond with the C−N bond. [d] Transition structure for methyl rotation.

C_2H, C_2H_3, and C_2H_5 with HNC, for which previous studies are generally rather less extensive.

Reaction of CH_3 with HNC. The CH_3CNH PES has recently been studied in detail by Wang et al.,[29] using B3-LYP/6-311++G(2d,2p) to obtain optimized geometries. Our own structures, as depicted in Figure 1, differ little from those obtained in the earlier work (although not all structures sought are common to the two studies). Relative energies, which in the investigation of Wang et al.[29] were obtained using the G3 protocol, also show good agreement (see Table 3): there are no discrepancies exceeding 6 kJ mol^{-1}.

It is apparent that the reaction of CH_3 + HNC is impeded by a substantial overall activation barrier on the entrance channel (barrier height = 31 kJ mol^{-1} (this work), 35 kJ mol^{-1}),[29] which will very effectively impede formation of the initial intermediate **Ia** at low temperatures. Furthermore, there is no real prospect for tunneling through this barrier in a manner analogous to that proposed for H + HNC,[26] for which the low-temperature reaction rate is expected to be nonnegligible despite the entrance channel barrier. The CH_3 entrance channel barrier is one of only two barriers that protrude above the total energy of reactants on that portion of the PES explored in the present work (other sizable barriers certainly exist, by perusal of the Wang et al.[29] study); therefore, at sufficiently high temperature to permit formation of **Ia**, fluxional interconversion with **Ib**, by either methyl group inversion or imine N−H inversion, will be facile (as will methyl group rotation, for which a very slight barrier is evident for both **Ia** and **Ib**). Ultimately, formation of acetonitrile as a product is the most probable bimolecular outcome from intermediate **I**; competing formation of HCN + CH_3, although more exothermic, is feasible only from intermediate **II** whose formation requires traversal of a somewhat larger barrier (**I/II**) than that which impedes the initial CH_3 + HNC entrance channel. Barriers to hydrogen cyanide and to acetonitrile formation from intermediate **II** are both submerged approximately 20 kJ mol^{-1} below the initial energy of reactants, suggesting comparable efficiency of formation of both sets of possible products from intermediate **II** (although a more reliable assessment could be obtained via an RRKM treatment or a similar approach).

The reaction of CH_3 with HNC is perhaps most pertinent to the upper atmospheric chemistry of the Saturnian moon Titan, where CH_3 and H are the most abundant radicals over the altitude range at which HNC is expected to occur in significant concentrations.[19] It is already accepted that the reaction of H with HNC is very inefficient at the relevant temperature of ∼200 K;[26,27] thus, it has been proposed that the reaction of CH_3 with HNC, producing acetonitrile, would if efficient constitute the predominant loss mechanism for HNC within Titan's ionosphere.[19] We can now assert with reasonable confidence that CH_3 will not significantly destroy HNC at these temperatures: it would appear, therefore, that the most important loss process for Titanian HNC will be via ion/molecule reactions, which have been identified as a viable alternative removal mechanism.[19]

Reaction of C_2H with HNC. Three previous studies by Osamura and co-workers[28,39,40] have explored various portions of the PES associated with this reaction. The first of these studies,[28] which employed CCSD(T)/cc-pVTZ//CISD/DZ+P calculations, provides a good platform for comparison with the present work since it was directly concerned with the mechanism of the C_2H + HNC reaction (among others). The second study,[39] concerning dissociation of HCCCNH as an indication of dissociative recombination pathways of HC_3NH^+ + e, also has some stationary points that are featured in the present work and uses B3-LYP/DZP as the method of geometry optimization (with single-point energies again obtained with CCSD(T)/cc-pVTZ). The third study, which involved a detailed exploration of the PES for the C_2H_2 + CN reaction,[40] is less relevant in the present context, since it includes few of the intermediate species dealt with in the present work.

Agreement between our relative energies (see Table 4) and those of Fukuzawa and Osamura[28] is often poor; there are discrepancies of 25 kJ mol^{-1} or more for the intermediate stationary points **I**, **I/B**, and **II/B**. One important point of accord is the apparent absence of a transition state on the C_2H + HNC entrance channel, although this arises for different reasons in the two studies. In the work of Fukuzawa and Osamura, an entrance channel transition state geometry is obtained by optimization at the CISD/DZ+P level but is found to lie below the total energy of reactants according to the subsequent CCSD(T) single-point calculations. In the present work, no entrance channel transition state exists at our default level of geometry optimization, viz. B3-LYP/6-311+G**. Such an **A/I** transition state structure can be located at the QCISD/6-31G* level, as indicated in Table 2, and when this geometry is characterized by the CBS-RAD protocol, we obtain a relative energy of −11.6 kJ mol^{-1}, which supports the assignment of a barrierless entrance channel and shows very good agreement with the

TABLE 4. Total Energies for Stationary Points on the [C_2H + HNC] Potential Energy Surface at the CBS-RAD Level of Theory

species	ZPE[a] (mHartree)	i[a]	$<S^2>$[a]	E_0[a] (Hartree)	E_{rel}[a] (kJ mol^{-1})	lit[a] (kJ mol^{-1})
R + CNH (**A**)			1.11		0	0
I[b]	35.43	0	1.13	−169.84182	−264.3	−236.8[c]
I/I (TS)[e]	33.15	1	1.14	−169.81775	−201.1	
I/B (TS)	27.70	1	1.31	−169.80018	−154.9	−115.9[c]
RCN + H (**B**)			0.75		−176.4	−157.7[c], −177[d]
I/II (TS)	30.59	1	1.10	−169.77845	−97.9	
II	36.17	0	1.21	−169.84268	−266.5	−266.9[c]
II/B (TS)	28.18	1	1.36	−169.79640	−145.0	−113.0[c]
II/C (TS)	31.80	1	1.17	−169.76298	−57.3	−56.1[c]
R + HCN (**C**)			1.11		−58.8	−62.8[c], −60[d]
A/III (TS)	28.72	1	1.14	−169.72992	29.5	13[d]
RH···CN (**III**)	32.43	0	1.13	−169.77570	−90.6	
RH + CN (**D**)			1.13		−82.3	−83[d]

[a] See footnotes *a*−*f* for Table 1. [b] Shown as structure **Ib** in Figure 1. [c] CCSD(T)/cc-pVTZ//CISD/DZ+P values, reported in ref 28. [d] B3-LYP/6-311G** values, reported in ref 38. [e] Shown as structure **Ia/Ib** (TS2) in Figure 1.

CCSD(T)/cc-PVTZ relative energy obtained for the corresponding "stationary point" in the earlier study.[28] Excellent agreement is also seen between our CBS-RAD value (+35.7 kJ mol^{-1}) and the previous CCSD(T)/cc-pVTZ//CISD/DZ+P value (+35.6 kJ mol^{-1})[28] for the relative energy of the entrance channel barrier to attack at the N atom; we therefore concur with Fukuzawa and Osamura that this channel, which leads to (exothermic) HCCNC formation, is not viable at interstellar cloud temperatures. Thus, while some large discrepancies are evident between the previous study[28] and the present work, there is no significant qualitative disagreement regarding the nature of the potential energy surface at the two different levels of theory employed. The differences in relative energy that are found most likely reflect the comparatively large extent of spin contamination in many of these stationary points,[41] for which the $<S^2>$ values are close to the most spin-contaminated examples used in the testing and development of the CBS-RAD methodology.[31]

The CCSD(T)/cc-pVTZ//B3-LYP/DZP study of Osamura et al.[39] includes the dissociation pathway **I** → **B**, which features also in the present work but does not report total energies for C_2H + HNC (which we have used, in Table 4, as the relative energy zero). If we compare relative energies for the **I** → **B** dissociation, we find that the **I/B** barrier lies 129.3 kJ mol^{-1} above **I**, with **B** 97.0 kJ mol^{-1} above **I**, according to Osamura et al.;[39] our corresponding values are, respectively, 109.4 and 87.9 kJ mol^{-1}. Again, discrepancies between methods appear greatest for the highly spin-contaminated transition structure.

The C_2H + HNC PES shows other features not encountered on the other R + HNC surfaces. First, we have not been able to isolate two stereoisomeric structures **Ia** and **Ib** on this surface. It appears that only one HCCCNH structure **I** exists as a local minimum. Second, the barrier for **I/II** isomerization in this instance lies very far below the initial energy of reactants, indicating that this isomerization can compete with H loss (channel **B**) from the local minimum **I**. Furthermore, both feasible dissociative channels from **II**—that is, formation of HCCCN + H (**B**) and HCN + C_2H (**C**)—are energetically accessible from the reactants, with no intervening absolute barriers. The potential for C_2H-catalyzed isomerization of HNC to HCN, in this manner, was not explored in the otherwise detailed study of Fukuzawa and Osamura.[28] Finally, the exothermicity of process **D**—formation of C_2H_2 + CN—has merited characterization of the intermediate stationary points, which indicate that a substantial barrier exists on this pathway, in qualitative agreement with the B3-LYP/6-311G** calculations of Huang et al.[40]

TABLE 5. Total Energies for Stationary Points on the [C_2H_3 + HNC] Potential Energy Surface at the CBS-RAD Level of Theory

species	ZPE[a] (mHartree)	i[a]	$<S^2>$[a]	E_0[a] (Hartree)	E_{rel}[a] (kJ mol^{-1})
R + CNH (**A**)			0.93		0
A/I (TS)	53.19	1	0.96	−170.99999	16.6
Ia[b]	59.24	0	1.07	−171.05760	−134.6
Ia/Ia (TS)[c]	59.15	1	1.11	−171.05343	−123.7
Ia/Ib (TS1)	57.10	2	1.15	−171.03824	−83.8
Ia/Ib (TS2)	58.20	1	0.88	−171.04000	−88.4
Ib[b]	60.28	0	1.07	−171.06525	−154.7
Ib/Ib (TS)[c]	60.11	1	1.12	−171.06115	−144.0
I/B (TS)	51.17	1	1.13	−171.02540	−50.1
RCN + H (**B**)			0.75		−81.2
I/II (TS)	54.79	1	1.05	−171.00640	−0.2
II	60.00	0	1.23	−171.07446	−178.9
II/B (TS)	51.96	1	1.19	−171.02830	−57.7
II/C (TS)	54.18	1	1.13	−171.02088	−38.2
R + HCN (**C**)			0.93		−58.8

[a] See footnotes *a*−*f* for Table 1. [b] Local minimum features a *trans*-CCCN configuration. [c] Transition structure for vinyl group rotation, featuring a *cis*-CCCN configuration.

The possibility of competition between the **I/II** and the **I/B** pathways on the exit channel implies that a detailed analysis, e.g., an RRKM treatment, is required to reliably determine the branching ratio for the C_2H + HNC reaction at even the lowest temperatures. However, because both of these processes fundamentally involve motion of the same hydrogen atom relative to the CCCN backbone, it would appear that the dissociative **I/B** pathway, possessing a substantially more deeply submerged barrier than the reversible **I/II** channel, will predominate; thus, we expect that the overall branching ratio for the reaction

$$HNC + C_2H \rightarrow HCCCN + H \quad (3a)$$

$$\rightarrow HCN + C_2H \quad (3b)$$

will very substantially favor 3a over 3b.[42] Therefore, as Fukuzawa and Osamura[28] have previously suggested, reaction 3 is potentially a very important route to HCCCN, an abundant molecule in cold, dark interstellar clouds.

Reaction of C_2H_3 with HNC. Our relative energies for the C_2H_3 + HNC PES are detailed in Table 5. This region of the C_3H_4N surface appears not to have been previously explored elsewhere, although a detailed exploration of another portion of this surface—connected with the mechanism for reaction of CN with C_2H_4—has been undertaken, at the B3-LYP/6-311G**

level of theory, by Balucani et al.[43] As in the case of the reaction of C_2H with HNC, we have chosen not to extend our exploration to this neighboring region, because of the expected low probability of C_2H_3 + HNC reactants accessing this portion of the PES in competition with more immediately available dissociative channels.

As another "unsaturated" radical, we might expect C_2H_3 to exhibit similar reactivity to that of C_2H with HNC. Instead, our characterization of the PES shows more similarity to the features seen on the surfaces for reaction of H and of CH_3 with HNC; namely, the reaction is found to be barrier-inhibited on the enrtance channel according to B3-LYP/6-311+G** calculations (and substantiated according to the CBS-RAD treatment of the B3-LYP geometries) without an accompanying absolute barrier on the exit channel to RCN (in this case, acrylonitrile) + H. Interconversion of **I** to **II** is impeded by a barrier that is essentially level with the initial energy of the reactants at 0 K (but 50 kJ mol^{-1} above the submerged dissociative barrier for production of C_2H_3CN from **I**); once **II** is formed, dissociation to both C_2H_3CN + H and C_2H_3 + HCN is energetically accessible at the initial energy of reactants.

Structurally, we find that according to B3-LYP/6-311+G** frequency calculations both the **Ia** and the **Ib** stereoisomeric local minima possess *trans*-CCCN backbones; optimization followed by frequency calculation on the corresponding *cis*-CCCN analogues reveals both the latter structures to be transition structures for vinyl group rotation, lying 9.9 and 10.7 kJ mol^{-1} above their respective minima at the CBS-RAD level. Interconversion of **Ia** and **Ib** is achieved by inversion of either the CCN or the CNH bond angle and appears equally facile (as judged by the energetic requirements) through either mode.

The degree of spin contamination evident in these stationary points is rather high, although less so than that seen for C_2H + HNC. Nevertheless, most of the "submerged" barriers here are sufficiently low-lying that it seems highly improbable that a more refined computational treatment would cause them to protrude above the reactants' combined total energies: the **I/II** isomerization barrier is an obvious exception, lying only 0.2 kJ mol^{-1} below the C_2H_3 + HNC reactants according to our CBS-RAD computations. The entrance channel barrier, lower than that seen for R = CH_3 but higher than for R = H, is scarcely affected by the choice of B3-LYP/6-311+G** or QCISD/6-31G* as the method of geometry optimization (see Table 2): this observation, and the general inference that B3-LYP geometries are more likely to lead to an underestimation rather than an overestimation of the true barrier height, additionally strengthen the allocation of a sizable entrance channel barrier as a genuine feature of the C_2H_3 + HNC reaction. It therefore seems that this reaction cannot serve as a significant precursor to the formation of acrylonitrile in environments such as dense interstellar clouds[44−47] and the atmosphere of the satellite Titan.[48]

Reaction of C_2H_5 with HNC. This surface, for which our calculated energetic parameters are summarized in Table 6, has not been explored previously. Barriers on the entrance channel and on the **I/II** isomerization pathway are sufficiently large (+30 and +52 kJ mol^{-1}, respectively) as to effectively prevent any real prospect for a low-temperature reaction between C_2H_5 and HNC. Moreover, the exit channel barrier (**I**/**B**) to ethyl cyanide formation is sufficiently close (−3.0 kJ mol^{-1}) to the reactants' total energy, at this level of theory, to suggest that an absolute barrier may also protrude on this exit channel.

As with C_2H_3CNH, both the *trans*-CCCN structures **Ia** and **Ib** are minima, while the *cis*-CCCN analogues are (ethyl group) rotational transition structures. However, a rather large number of asymmetric rotational conformers also bear consideration as stationary points; while not having attempted to explicitly characterize all of the possible (ethyl and methyl) rotational transition states, we have established that two different chiral local minima, corresponding to the gauche-CCCN conformations of **Ia** and **Ib**, also exist. These species, which lie, respectively, 1.7 (**Ia**-gauche) and 4.9 kJ mol^{-1} (**Ib**-gauche) above the corresponding *trans*-CCCN conformers, are separated from the latter structures by rotational barriers not exceeding about 7 kJ mol^{-1} above the energy of the relevant *trans*-CCCN minimum. As with C_2H_3CNH (and CH_3CNH and HCNH) also, interconversion of **Ia** and **Ib** is achieved by either CCN or CNH bond inversion, both of which appear highly accessible at the total energy of reactants.

TABLE 6. Total Energies for Stationary Points on the [C_2H_5 + HNC] Potential Energy Surface at the CBS-RAD Level of Theory

species	ZPE[a] (mHartree)	i[a]	$<S^2>$[a]	E_0[a] (Hartree)	E_{rel}[a] (kJ mol^{-1})
R + CNH (**A**)			0.76		0
A/I (TS)	77.06	1	0.79	−172.22337	29.6
Ia[b,c]	82.88	0	0.81	−172.26538	−80.7
Ia/Ib (TS1)	80.49	1	0.81	−172.24757	−33.9
Ia/Ib (TS2)	81.60	1	0.77	−172.24771	−34.3
Ib[b,c]	83.73	0	0.80	−172.27272	−100.0
I/B (TS)	74.88	1	0.85	−172.23580	−3.0
RCN + H (**B**)			0.75		−38.3
I/II (TS)	78.17	1	0.79	−172.21479	52.1
II	83.10	0	0.90	−172.28190	−124.1
II/B (TS)	75.48	1	0.89	−172.23972	−13.3
II/C (TS)	78.11	1	0.99	−172.24479	−26.6
R + HCN (**C**)			0.76		−58.8

[a] See footnotes *a*−*e* for Table 1. [b] Local minimum features a *trans*-CCCN configuration. [c] An alternative local minimum, featuring the same RCNH configuration but with a gauche CC−CN conformation, is <5 kJ mol^{-1} higher in energy.

General Discussion of Observed Trends. As noted in a preceding section, the relative energies for reaction of saturated radicals R (H, CH_3, C_2H_5) are sufficiently consistent to allow the construction of the useful generalized surface shown in Figure 2. The adherence of the vinyl radical to such a generalized surface is also reasonable, except that the entrance channel barrier height is very substantially underestimated by such a model, while the C_2H_3 + HNC dissociative barriers **I**/**B** and **II**/**C** are somewhat overestimated by the generalized surface when assessed against our CBS-RAD values for these species. The CBS-RAD potential energy surface for C_2H + HNC does not adhere well to the model shown in Figure 2. It appears, therefore, that the reactivity of unsaturated radicals with HNC should properly be assessed on a case-by-case basis.

What does our model say of the reactivity of larger saturated alkyl radicals with HNC? The H, CH_3, and C_2H_5 radicals surveyed here are all primary radicals and consequently have innately little stabilization of the radical center: progressively greater degrees of radical stabilization are expected for secondary (e.g., $(CH_3)_2CH$) and tertiary (e.g., $(CH_3)_3C$) radicals. The model shown in Figure 2 indicates that the height of any R + HNC entrance channel barrier is dependent on the relative energies of R + HNC (**A**) and of the intermediate RCNH (**Ib**), that is, effectively, a dependence on the R−CNH bond strength. We predict that if this bond strength exceeds about 134 kJ mol^{-1}, the entrance channel barrier will be submerged below the initial energy of reactants (permitting occurrence of the reaction at all temperatures). For our series of prototypical alkyl radicals H, CH_3, and C_2H_5, this crucial bond strength has values of 129.4,

TABLE 7. Entrance Channel Barriers for Addition at C or at N of HNC and at C of HCN at the CBS-RAD Level of Theory

R	E_a(R−CNH)[a,b] (kJ mol^{-1})	E_a(R−N(H)C)[a,c] (kJ mol^{-1})	E_a(R−C(H)N)[a,d] (kJ mol^{-1})
H	8.0	58.9	22.7
CH_3	30.5	92.9	36.0
C_2H	0	35.7	1.5
C_2H_3	16.6	69.5	20.6
C_2H_5	29.6	84.2	32.2

[a] Activation energy barrier (at 0 K), including zero-point vibrational energy. [b] Barrier for addition at C of HNC relative to total energy of the reactants R + HNC. [c] Barrier for addition at N of HNC relative to total energy of the reactants R + HNC. [d] Barrier for addition at C of HCN relative to total energy of the reactants R + HCN.

106.1, and 100.0 kJ mol^{-1}, respectively. The R−CNH bond strength for larger primary radicals is likely to closely parallel that for the methyl and the ethyl radical, while for secondary and tertiary alkyl radicals it would appear that the R−CNH bond should be rather weaker because of the greater loss in alkyl radical stabilization upon combination of R with HNC. We surmise, therefore, that the existence of a significant ($E_a \geq 10$ kJ mol^{-1}) activation energy barrier will be a universal feature on the PES of saturated alkyl radicals R reacting with HNC: thus, no such reactions will be capable of low-temperature (bimolecular) depletion of HNC.

Entrance channel barriers for R + HNC, for attack at the terminal C atom and at N, are summarized in Table 7. Comparison of the C atom and N atom barriers shows plainly that competition from N atom attack should not impinge significantly on the occurrence of addition to the terminal carbon of HNC, except at particularly elevated temperatures (where, in any event, unimolecular isomerization of HNC to HCN will be an important loss process). With the exception of R = C_2H, where addition to C of HNC lacks a barrier, the entrance channel for addition at N is always impeded by a barrier at least 50 kJ mol^{-1} larger than that obtruding addition at C. This disparity, and the general endothermicity of product formation directly resulting from addition at the N of HNC, suggests that the exploration of PES features lying beyond the N addition barrier is of little practical relevance.

The PES explored here also provide some information on the reactivity of R with HCN, as indicated in Table 7. Previous studies have established that the reactions of H,[26,27] CH_3,[29] and C_2H[28] with HCN are barrier-inhibited, over and above any reaction endothermicity (in fact, of these cases, only formation of HCCCN + H is exothermic, in the reaction of C_2H with HCN). The existence of absolute barriers for these reactions is supported by our results, although the barrier found for C_2H + HCN is very small: within the expected limited accuracy of the CBS-RAD method, it is highly possible that the apparent barrier for C_2H + HCN is not genuine. Other barriers, of >20 kJ mol^{-1} in all other cases explored here, are more secure: the reactions of C_2H_3 + HCN and of C_2H_5 + HCN appear not to have been studied previously, and it is significant to note that the reaction of the vinyl radical, which provides an exothermic pathway to acrylonitrile, C_2H_3CN, is not viable at low temperatures. We note also that in all instances, the entrance channel barriers for R + HCN (leading to intermediate **II**) are slightly higher than the corresponding entrance channel barriers for R + HNC (leading to intermediate **I**). Thus, as chemical intuition would tell us, HNC is indeed the more reactive species. It may, however, appear somewhat surprising that for a given radical R, the difference between HNC and HCN entrance channel barrier heights is so small; the barrier "protecting" HCN is usually less than 10 kJ mol^{-1} larger than that for HNC. This touches on an enduring conundrum in interstellar chemistry: both HCN and HNC are widely seen interstellar molecules, probably with broadly comparable total rates of production, yet at $T = 20$ K and below the abundance of HNC is generally found to exceed that of HCN.[10] The HNC/HCN ratio drops as T increases, in a manner suggestive of some unknown HNC loss process having an activation energy of 200 K (1.7 kJ mol^{-1}).[10] Can we identify such a loss process among the reactions of HNC with the hydrocarbon radicals? On the basis of the present study, it would appear not; thus, this remains a mystery to be uncovered, perhaps by further study.

Conclusions

The PES for reactions of small hydrocarbon radicals with HNC show generally similar features, according to our CBS-RAD calculations. In most cases, reaction proceeds (after traversal of an entrance channel barrier) through formation of an initial intermediate with a *cis*-RCNH configuration, with a readily surmounted barrier leading to a more stable *trans*-RCNH form. Further isomerization to a yet lower-energy structure RC(H)N is possible, but for R = H, CH_3, and C_2H_5, the barrier to this isomerization lies above the initial energy of the reactants R + HNC.

Of the radicals H, CH_3, C_2H, C_2H_3, and C_2H_5, only C_2H is apparently capable of reacting with HNC at low temperature, with a likely major product channel of HCCCN + H but with access also to the C_2H + HCN product channel. The corresponding reactions of R + HCN are consistently attended by somewhat larger entrance channel barriers than R + HNC, but the C_2H + HCN entrance channel barrier is very low and may not be a genuine feature.

Acknowledgment. We thank the School of Chemistry, University College (UNSW, ADFA) for continued access to the workstations used in the calculation of these results.

References and Notes

(1) Lizst, H. S.; Lucas, R. *Astron. Astrophys.* **2001**, *370*, 576.
(2) Turner, B. E.; Pirogov, L.; Minh, Y. C. *Astrophys. J.* **1997**, *483*, 235.
(3) Dutrey, A.; Guilloteau, S.; Guelin, M. *Astron. Astrophys.* **1997**, *317*, L55.
(4) Dartois, E.; Gerin, M.; d'Hendecourt, L. *Astron. Astrophys.* **2000**, *361*, 1095.
(5) Bieging, J. H.; Rieu, N.-Q. *Astrophys. J.* **1989**, *329*, L107.
(6) Bujarrabal, V.; Fuente, A.; Omont, A. *Astron. Astrophys.* **1994**, *285*, 247.
(7) Cox, P.; Omont, A.; Huggins, P. J.; Bachiller, R.; Forveille, T. *Astron. Astrophys.* **1992**, *266*, 420.
(8) Fukasaku, S.; Hirahara, Y.; Masuda, A.; Kawaguchi, K.; Ishikawa, S.-I.; Kaifu, N.; Irvine, W. M. *Astrophys. J.* **1994**, *437*, 410.
(9) Pratap, P.; Dickens, J. E.; Snell, R. L.; Miralles, M. P.; Bergin, E. A.; Irvine, W. M.; Schloerb, F. P. *Astrophys. J.* **1997**, *486*, 862.
(10) Hirota, T.; Yamamoto, S.; Mikami, H.; Ohishi, M. *Astrophys. J.* **1998**, *503*, 717.
(11) Hirota, T.; Ikeda, M.; Yamamoto, S. *Astrophys. J.* **2001**, *547*, 814.
(12) Lis, D. C.; Keene, J.; Young, K.; Phillips, T. G.; Bockelée-Morvan, D.; Crovisier, J.; Schilke, P.; Goldsmith, P. F.; Bergin, E. A. *Icarus* **1997**, *130*, 355.
(13) Irvine, W. M.; Bergin, E. A.; Dickens, J. E.; Jewitt, D.; Lovell, A. J.; Matthews, H. E.; Schloerb, F. P.; Senay, M. *Nature* **1998**, *393*, 547.
(14) Hirota, T.; Yamamoto, S.; Kawaguchi, K.; Sakamoto, A.; Ukita, N. *Astrophys. J.* **1999**, *520*, 895.
(15) Ziurys, L. M.; Savage, C.; Brewster, M. A.; Apponi, A. J.; Pesch, T. C.; Wyckoff, S. *Astrophys. J.* **1999**, *527*, L67.
(16) Biver, N.; Bockelée-Morvan, D.; Crovisier, J.; Henry, F.; Davies, J. K.; Matthews, H. E.; Colom, P.; Gérard, E.; Lis, D. C.; Phillips, T. G. *Astron. J.* **2000**, *120*, 1554.

(17) Bockelée-Morvan, D.; Biver, N.; Moreno, R.; Colom, P.; Crovisier, J.; Gérard, E.; Henry, F.; Lis, D.; Matthews, H. E.; Weaver, H. A.; Womack, M.; Festou, M. C. *Science* **2001**, *292*, 1339.

(18) Rodgers, S. D.; Charnley, S. B. *Mon. Not. R. Astron. Soc.* **2001**, *323*, 84.

(19) Petrie, S. *Icarus* **2001**, *151*, 196.

(20) Shiba, Y.; Hirano, T.; Nagashima, U.; Ishii, K. *J. Chem. Phys.* **1998**, *108*, 698.

(21) Talbi, D.; Ellinger, Y. *Chem. Phys. Lett.* **1998**, *288*, 155.

(22) Jursic, B. S. *J. Mol. Struct. (THEOCHEM)* **1999**, *487*, 211.

(23) Tachikawa, H. *Phys. Chem. Chem. Phys.* **1999**, *1*, 4925.

(24) Semaniak, J.; Minaev, B. F.; Derkatch, A. M.; Hellberg, F.; Neau, A.; Rosén, S.; Thomas, R.; Larsson, M.; Danared, H.; Paál, A.; af Ugglas, M. *Astrophys. J. Suppl. Ser.* **2001**, *135*, 275.

(25) Lin, M. C.; He, Y.; Melius, C. F. *Int. J. Chem. Kinet.* **1992**, *24*, 1103.

(26) Talbi, D.; Ellinger, Y.; Herbst, E. *Astron. Astrophys.* **1996**, *314*, 688.

(27) Sumathi, R.; Nguyen, M. T. *J. Phys. Chem. A* **1998**, *102*, 8013.

(28) Fukuzawa, K.; Osamura, Y. *Astrophys. J.* **1997**, *489*, 113.

(29) Wang, B.; Hou, H.; Gu, Y. *J. Phys. Chem. A* **2001**, *105*, 156.

(30) Byrd, E. F. C.; Sherrill, C. D.; Head-Gordon, M. *J. Phys. Chem. A* **2001**, *105*, 9736.

(31) Mayer, P. M.; Parkinson, C. J.; Smith, D. M.; Radom, L. *J. Chem. Phys.* **1998**, *108*, 604.

(32) Ochterski, J. W.; Petersson, G. A.; Montgomery, J. A., Jr. *J. Chem. Phys.* **1996**, *104*, 2598.

(33) Henry, D. J.; Parkinson, C. J.; Radom, L. *J. Phys. Chem. A* **2002**, *106*, 7927.

(34) Frisch, M. J.; Trucks, G. W.; Schegel, H. B.; Scuseria, G. E.; Robb, M. A.; Cheeseman, J. R.; Zakrzewski, V. G.; Montgomery, J. A., Jr.; Stratmann, R. E.; Burant, J. C.; Dapprich, S.; Millam, J. M.; Daniels, A. D.; Kudin, K. N.; Strain, M. C.; Farkas, O.; Tomasi, J.; Barone, V.; Cossi, M.; Cammi, R.; Mennucci, B.; Pomelli, C.; Adamo, C.; Clifford, S.; Ochterski, J. W.; Petersson, G. A.; Ayala, P. Y.; Cui, Q.; Morokuma, K.; Malick, D. K.; Rabuck, A. D.; Raghavachari, K.; Foresman, J. B.; Cioslowski, J.; Ortiz, J. V.; Stefanov, B. B.; Liu, G.; Liashenko, A.; Piskorz, P.; Komaromi, I.; Gomperts, R.; Martin, R. L.; Fox, D. J.; Keith, T.; Al-Laham, M. A.; Peng, C. Y.; Nanayakkara, A.; Gonzalez, C.; Challacombe, M.; Gill, P. M. W.; Johnson, B. G.; Chen, W.; Wong, M. W.; Andres, J. L.; Head-Gordon, M.; Replogle, E. S.; Pople, J. A.; Gaussian, Inc.: Pittsburgh, PA, 1998.

(35) For R = CH_3, C_2H_3, and C_2H_5, at least two conformers exist as stationary points for each of the structures shown.

(36) Gonzales, J. M.; Cox, R. S.; Brown, S. T.; Allen, W. D.; Schaefer, H. F., III. *J. Phys. Chem. A* **2001**, *105*, 11327.

(37) Lynch, B. J.; Truhlar, D. G. *J. Phys. Chem. A* **2001**, *105*, 2936.

(38) Poater, J.; Sola, M.; Duran, M.; Robles, J. *Phys. Chem. Chem. Phys.* **2002**, *4*, 722.

(39) Osamura, Y.; Fukuzawa, K.; Terzieva, R.; Herbst, E. *Astrophys. J.* **1999**, *519*, 697.

(40) Huang, L. C. L.; Asvany, O.; Chang, A. H. H.; Balucani, N.; Lin, S. H.; Lee, Y. T.; Kaiser, R. I.; Osamura, Y. *J. Chem. Phys.* **2000**, *113*, 8656.

(41) An alternative influence on the calculated relative energies, that of the level of theory used for optimization of stationary points, has been assessed in some measure for this PES by performing an optimization of structure **I** at the QCISD/6-31G* level of theory: this yields a geometry rather closer to that obtained with CISD/DZ+P, reported in ref 28. Despite comparatively large differences in our QCISD/6-31G* and B3-LYP/6-311+G** optimized bond lengths for structure **I**, the difference in CBS-RAD total energies obtained for these two geometries is only 2.5 kJ mol^{-1}, implying that the major source of the ~28 kJ mol^{-1} discrepancy between the CCSD(T) results and our CBS-RAD values lies with the single-point energies rather than with the optimized geometries.

(42) The apparent comparative facility of dissociation of both **I** and **II** to HCCCN + H is also a factor in our decision, in the present work, not to examine pathways from structure **II** to the portion of the PES, which has been characterized by Huang et al.[40] at the B3-LYP/6-311G** level. We surmise that almost all **I** initially formed from C_2H + HNC will dissociate, either directly or via intermediate **II**, before this more remote region of the PES can be accessed. Furthermore, Huang et al.[40] have concluded that the sole significant product channel on this surface is, again, HCCCN + H.

(43) Balucani, N.; Asvany, O.; Chang, A. H. H.; Lin, S. H.; Lee, Y. T.; Kaiser, R. I.; Osamura, Y. *J. Chem. Phys.* **2000**, *113*, 8643.

(44) Gardner, F. F.; Winnewisser, G. *Astrophys. J.* **1975**, *195*, L127.

(45) Matthews, H. E.; Sears, T. J. *Astrophys. J.* **1983**, *272*, 149.

(46) Petrie, S.; Freeman, C. G.; McEwan, M. J. *Mon. Not. R. Astron. Soc.* **1992**, *257*, 438.

(47) Nummelin, A.; Bergman, P. *Astron. Astrophys.* **1999**, *341*, L59.

(48) Thompson, W. R.; Henry, T. J.; Schwartz, J. M.; Khare, B. N.; Sagan, C. *Icarus* **1991**, *90*, 57.